1

Electromagnetic Interference and Shielding

1.1 Introduction

Telecommunication devices and microelectronics inadvertently receive, generate, and/or propagate electromagnetic waves (EMWs) in a wide frequency range. Technological advancements toward smaller and smarter electronic devices have inevitably been accompanied by increased electromagnetic interference (EMI). EMI is a type of cross-talk between different devices and circuits operating in close proximity. This disrupting phenomenon often results in critical component malfunctioning, device underperformance, data loss, and incorrect signal interpretation [1–5]. More broadly, EMI is a serious concern for the aviation industry, including military jets, warships, and other strategic components, and can place a country's security at risk [6, 7]. The smallest error resulting from incorrect signal generation or interpretation could have serious consequences because of the false triggering of ammunition. Additionally, the increasing density of EMWs has a significant impact on human health [8, 9].

In the era of emerging fifth generation (5G) technology, the number of electronic devices and gadgets will increase drastically, resulting in increased exposure to wireless fidelity (Wi-Fi) and the internet of things (IoTs), as well as spreading electromagnetic terrorism and offensive information warfare [10]. Therefore, it is necessary to protect humans and electronic devices from the detrimental effects of EMI by providing suitable shielding. Thus, advanced EMI shielding materials should be developed to meet the challenges of advanced technologies.

The energy of EMWs can be attenuated by reflection, absorption, and multiple reflection mechanisms [11–13]. The primary mechanism involves the reflection of EMWs that strike the surface of a shielding material [2]. Highly conductive materials with excess mobile charge carriers (holes and/or electrons) show strong reflection upon interaction with electromagnetic radiation. Metals (e.g. Ag, Cu, and Al), which are the most conductive materials, show excellent EMI shielding properties through reflection, and have been used for decades in commercial appliances [14–16].

The second mechanism involves the absorption of EMWs within a shielding material. When EMWs propagate in a shielding material, their intensity is exponentially attenuated with the thickness. For efficient absorption, the electrical conductivity,

Two-Dimensional Materials for Electromagnetic Shielding, First Edition.
Chong Min Koo, Pradeep Sambyal, Aamir Iqbal, Faisal Shahzad, and Junpyo Hong.

dielectric permittivity, and magnetic permeability of the shielding material play a vital role in attenuating the energy of EMWs through Ohmic loss, dielectric loss, and magnetic loss, respectively [17–20].

The third mechanism involves multiple reflections that occur because of either thin thickness or the presence of multiple interfaces within the material. These types of multiple reflections are different and hence perform differently. When the thickness of a material is smaller than the skin depth, multiple reflections will decrease the total EMI shielding effectiveness (SE) value [12, 21], whereas this effect is negligible when the thickness of the material is larger than the skin depth. The skin depth is the thickness of the material at which the intensity of the incident EMWs falls by a value of $1/e$. In contrast, multiple reflections caused by the presence of multiple internal interfaces have a positive impact on the EMI SE value, as the internal scattering of EMWs from the internal interfaces will increase absorption and hence the EMI shielding ability of the material. A comprehensive description of each mechanism along with the influencing and controlling parameters is provided in Chapter 2.

1.2 Electromagnetic Field Sources and Impact on Human Beings

The innovation race is backed by advances in technology, which are marvelous in facilitating human life. Global technologies, including artificial intelligence (AI), automation, and IoT, provide services that affect every aspect of life. However, this emerging technology can also place human life at risk. The operating frequencies in the electromagnetic spectrum can be divided into two categories depending on potential hazards: ionizing and nonionizing (Figure 1.1). As the risks of high-frequency ionizing electromagnetic (EM) radiation, including X-rays and gamma cosmic rays, are well known, safety protocols have been developed to avoid any kind of exposure. Unfortunately, nonionizing low-frequency EMWs are a silent killer for humans and operating systems if left unattended. Currently, the most commonly used electronic device that operates in this frequency range is the cellular phone, the use of which has grown dramatically since the start of commercial services in 1983 [22]. In the first decade, the number of cellular users in the United States only reached ~2 million. However, there are now nearly 3 billion global users, and this number is expected to hit 6.1 billion in 2020 [22]. Although cellular phones and handheld devices transmit very low powers of 0.6 W while operating at 850 MHz to 3.5 GHz or even higher frequency, their frequent use in close proximity to the body is associated with severe health outcomes. Therefore, proper shielding of the field is required for a healthy work environment.

We are always surrounded by betraying electromagnetic fields. Generally, an alternating electric field generates a magnetic field around it, and vice versa. To apply appropriate shielding, it is essential to know about the sources that generate electromagnetic fields. These sources can be either natural or artificial (manmade).

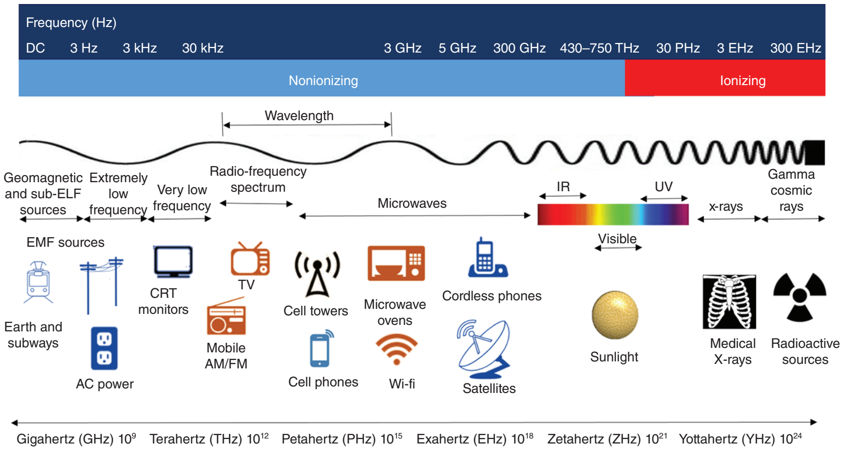

Figure 1.1 Frequency and wavelength ranges in the electromagnetic spectrum, and devices that emit radiation at certain frequencies. Source: Chong Min Koo.

1.2.1 Natural Sources

Generally, the Sun is the biggest source of electromagnetic radiation. Solar energy, which is the energy that reaches Earth from the Sun, consists of electromagnetic radiation at all wavelengths. Almost half of the radiation (49%) is in the low-frequency (longer wavelength) region, 44% in the visible region, which can be seen by the naked eye, and the remaining 7% in the high-frequency (shorter wavelength) ultraviolet region. This ionizing radiation is harmful to human skin and eyes, as well as the brain and various cells. In addition, the Earth, thunderstorms, and lightning also create strong electromagnetic fields. Earth's own magnetic field is strong enough to rotate a compass needle in the north–south direction. However, the generated geomagnetic field has a low frequency (1–300 Hz) with a power of 60 μT at the North/South poles and 30 μT at the equator [23]. Thunderstorms and lightning also produce electric fields by building up electrically charged particles in the atmosphere.

1.2.2 Artificial (Manmade) Sources

In the era of technology, all electrical or electronic devices used in everyday life (e.g. mini power sockets) generate electromagnetic radiation or require electromagnetic fields to function. Power lines and electronic equipment, including vacuum cleaners and hair dryers, are sources of low-frequency radiation with a power of approximately 17.44–164.75 μT when measured at a distance of 5 cm [23]. In contrast, radio stations, television antennas, mobile electronic devices, microwave ovens, and most importantly medical equipment generate high-frequency EMWs (100 kHz to 300 GHz). Typically, the radiation emitted from manmade sources is polarized, as it is produced by electromagnetic oscillation circuits. As polarized electromagnetic radiation can penetrate the human body, it is used in biomedical applications. However, exposure to such radiation above a certain limit is potentially deleterious to cells and tissues [24].

1.2.3 Effects on Human Health

We are surrounded by electromagnetic fields that have inevitably become a formidable part of our life. Initially, these fields were considered too weak to affect the biomolecular systems of humans and not strong enough to influence physiological functions. However, exposure to electromagnetic radiation can have a dreadful impact on human health. Some individuals are very sensitive to electromagnetic fields and show the symptoms of health disorders under mild exposure. This adverse phenomenon, called electromagnetic hypersensitivity (EHS), affects 1–3% of the global population, as reported by the WHO [25]. The observed symptoms include headaches, sleep disorders, dizziness, depression, palpitations, hot flushes, sweating, tinnitus, fatigue, limb pain, back pain, heart disease, tremors, nervousness, nausea, skin rashes, weakness, loss of appetite, and breathing difficulties [26]. Furthermore, sleep disorders and deficiencies have been observed in inhabitants close to electromagnetic radiation emitters, although several studies have also found otherwise. A case study found psychological symptoms such as depression, unmanageable emotions, and suicide among residents exposed to the 50 Hz chronic frequency of high-voltage power stations and highlighted an increased suicide (attempt) rate, most likely because of depression [27].

The ear is the first organ to be exposed to the electromagnetic radiation emitted by cellular phones, and a study reported that exposure to electromagnetic radiation of 50 Hz at an intensity of 4.45 pT may cause adverse auditory effects in humans [28]. The cochlear outer hair cells are vulnerable to injuries from exogenous and endogenous agents and electromagnetic radiation. To numerically analyze the specific absorption rate (SAR) along with heat transfer in the human eye, Wessapan and Rattanadecho exposed a human eye model to an electromagnetic field of 900–1800 MHz [29]. This study revealed heat and mass transfer phenomena in the eye under exposure to electromagnetic fields, with the highest SAR observed in the cornea. Lower frequencies affected the anterior chamber, whereas higher frequencies increased the temperature in the vitreous. The exposure time also strongly influenced the temperature increase in the human eye. These results demonstrate the fatal effects of electromagnetic fields on the visual performance of the human eye.

Epidemiological investigations have shown that electromagnetic radiation is carcinogenic to humans, with long exposure causing tumor development. These effects are more apparent in newborns. Studies on the effects of electromagnetic radiation on the nervous tissues have found that high-intensity radio frequency (RF) exposure affects the central nervous systems, brain chemistry, and blood–brain linkages in animals. Lowered concentrations of dopamine, epinephrine, and norepinephrine in the brain are associated with electromagnetic radiation. Ghione et al. experimentally observed altered nociception and cardiovascular abnormalities in a human head

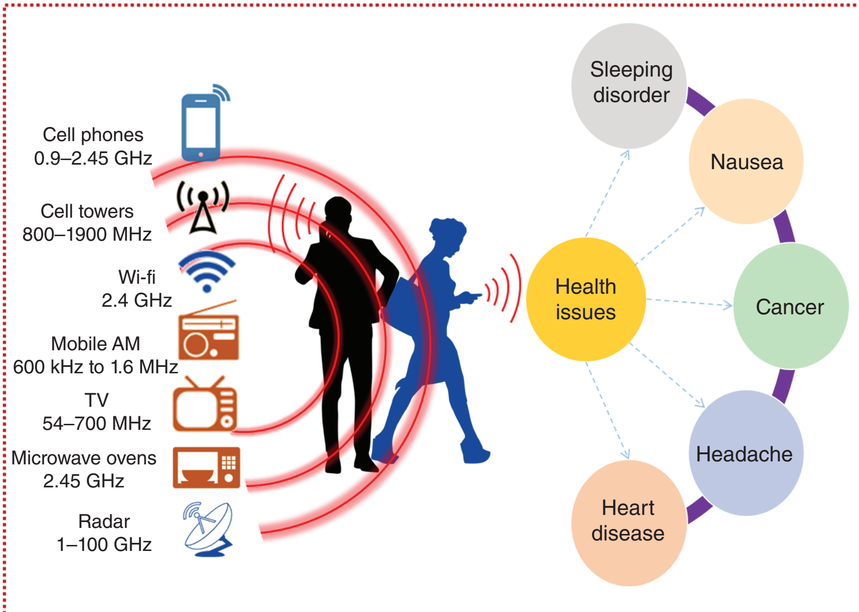

Figure 1.2 EMW sources and their potential harmful effects on humans. Source: Chong Min Koo.

exposed to electromagnetic radiation of 37 Hz with a flux density of 80 μT [30]. When placed close to the location of the heart in the chest, betrayed electromagnetic fields could also interfere with implanted pacemakers by altering heartbeats. Importantly, decreased male fertility is also linked with exposure to electromagnetic fields. Cellular phones have become an integral part of everyday life and are carried in pockets, very close to the reproductive system. Therefore, it is particularly important to investigate the potential effects of operating frequency and power. In a study on rats, various histopathological alterations, such as necrosis, focal tubular atrophy, and seminiferous epithelial erosion, were recorded under low-frequency exposure at 50 Hz; however, the serum testosterone level was barely affected [31]. Figure 1.2 summarizes various EMW sources along with their potential detrimental effects on human health.

Therefore, a practical way to safeguard humans is to follow the ALARA (as low as reasonably achievable) principle by maintaining a safe distance and minimizing exposure or to take other precautionary steps such as efficient shielding to attenuate the energy of EMWs. As maintaining a safe distance is practically impossible, the shielding strategy has emerged as a potential solution.

1.3 EMI Hazards for Data Security

EMI is a phenomenon in which the electromagnetic radiation from one electronic device disrupts other nearby electronic circuits via conduction or radiation transfer.

A severe EMI scenario can adversely affect the entire electronic system, causing device malfunction or system failure. This effect is quite strong in medical equipment, where electromagnetic radiation is used for biomedical applications and imaging. Consequently, the figures and/or results are affected if effective shielding is not provided. Low-frequency EMI caused by power sources can also have harmful effects on the hardware, resulting in data corruption or complete reformatting of the hard disk in severe cases. As a result, retrieving information from wireless terminals becomes impossible. Although EMI is unintentional most of the time, it can be misused in electronic warfare in the form of data loss, data hacking, radio jamming, security breaches, and other types of disturbances. Therefore, the defense department of a country strictly deals with disastrous EMI by following special shielding protocols.

1.4 Economic Aspects and the Global Market for EMI Shielding

From an application point of view, the market for EMI shielding materials can be categorized into different areas, including electronics, defense, aerospace, automotive, telecommunications, and medical appliances. Electronics hold a substantial market share because advanced compact and fast devices use efficient circuits that operate at higher frequencies. The second highest market share belongs to the defense sector, with applications including sophisticated satellites, radar equipment, and spacecraft. Countries are continuously increasing their defense budgets for the research and development of new arms and weapons, thus increasing global defense expenditures and contributing to a larger electromagnetic absorption and shielding market. In 2015, global military expenditures were approximately US$ 1.5 trillion, led by the United States, China, and Saudi Arabia (see Figure 1.3a for other countries). The aerospace industry is also growing with various ongoing space exploration missions. Furthermore, nearly 30 000 new passenger aircraft will be added to those currently in service over the next 20 years; hence, EMI shielding materials will be in high demand. Similarly, telecommunication devices, AI, IoT, and the automotive industry are expected to thrive in the coming years, leading to an ever-increasing demand for EMI shielding materials.

The global EMI shielding market has a projected size of US$ 6.8 billion in 2020 and is expected to reach US$ 9.2 billion by 2025, with a compound annual growth rate of 6.3% over the next five years (Figure 1.3b) [32]. Thus, there is a huge demand for the research and development of novel and efficient materials to meet stringent EMI shielding requirements.

1.5 Electromagnetic Compatibility Regulations and Standards

Over the past few decades, the increase in electrical and electronic systems with their accompanying electromagnetic pollution has necessitated the creation and

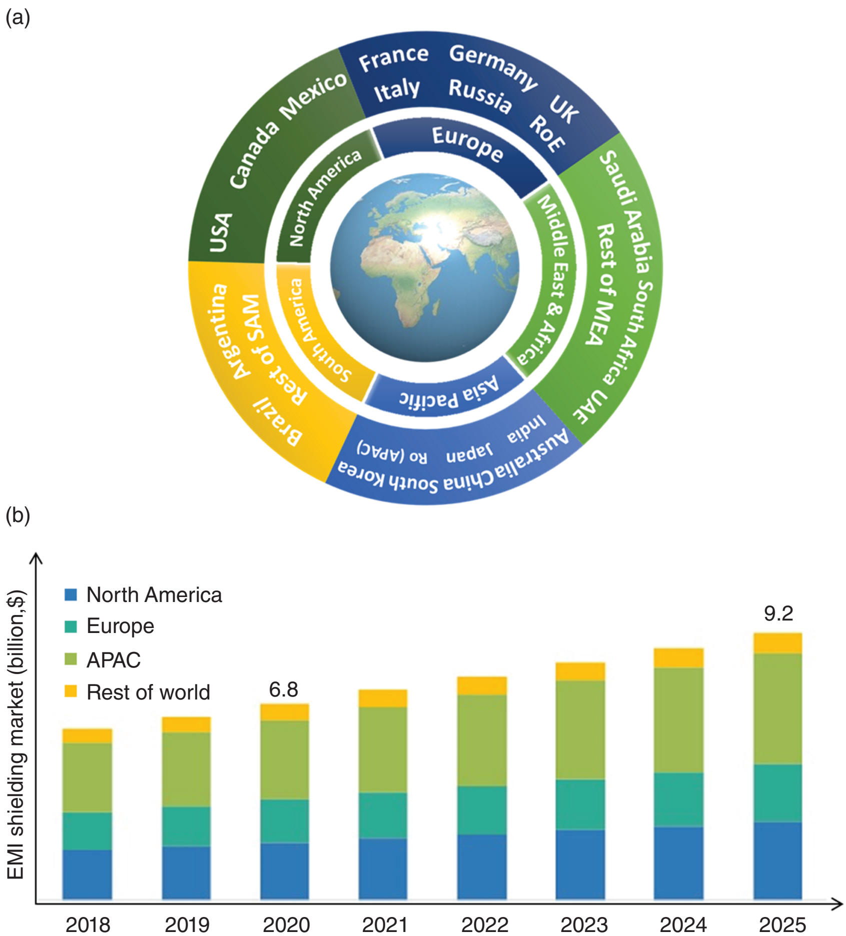

Figure 1.3 (a) Global market shares in the field of EMI shielding and (b) global market over the next five years. Source: https://www.marketsandmarkets.com/Market-Reports/emi-shielding-market-105681800.html.

implementation of electromagnetic compatibility (EMC) standards around the globe (Figure 1.4). Historically, during World War II, EMC became very important in the defense sector, as mission success was highly reliant on electronic communication systems, which is still the case today. In the civil sector, the extensive use of radio facilities, modern gadgets, telecommunications, and electric systems has spread EMI pollution. Therefore, a set of standards is required so that the products or systems applied in the civil, defense, and industry sectors are immune to external EMI pollution and do not generate high electromagnetic radiation.

Compiling all existing standards and creating a set of documents as a recommendation for EMC is tedious, as every nation has its own set of standards for instruments, procedures, and limits. The most renowned international organizations are the International Standard Organization (ISO) and the International Electrotechnical Commission (IEC). Alongside these two agencies, many other

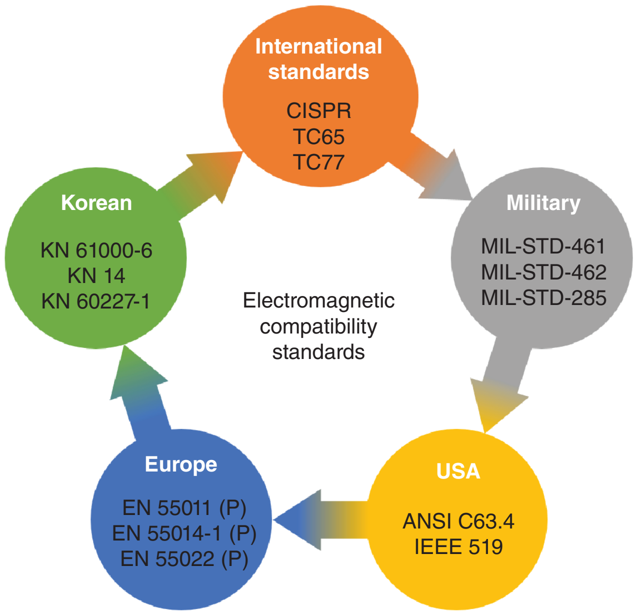

Figure 1.4 Summary of global standards and limitations for the safe use of electrical and electronic equipment. Source: Chong Min Koo.

agencies, such as the European Committee for Electrotechnical Standardization (CENELEC) in Europe, the Federal Communications Commission (FCC) in the United States, and the Korean EMC standards (KSC) in Korea, publish national standards for use in the civilian segment and military or defense standards (MIL-STD) for use in the military segment [33].

1.5.1 International Standards

The IEC, which is the organization that monitors EMC standards and testing procedures, comprises three technical committees on EMC, namely, CISPR (International Special Committee on Radio Interference), TC65 (related to the immunity standards), and TC77 (related to EMC in electrical systems and networks). CISPR compiles their findings related to EMC issues in the form of standards labeled CISPR10–CISPR23. TC65 provides standards related to immunity under designation 801. TC77 provides standards related to low-frequency phenomena in the power network, such as harmonics and flicker, under designations 555 and 1000, respectively. The CISPR22 standards are the basic foundation of the national standards of several countries for emission from IT or communication systems. Owing to variations in the prerequisites of various countries, the standards suggested by CISPR cannot be implemented as law. However, in accordance with the will of each nation, these standards can be implemented or modified as national standards [34].

1.5.2 FCC Standards (United States)

In the United States, radio and wired communications and interference are regulated by the FCC. Any equipment that is imported to or sold in the United States must fulfill the standards laid out by the FCC. The FCC rules and regulations deal with EMC standards, measurement methods American National Standards Institute (ANSI C63.4), equipment or product approval processes, and marking requirements. Three sections deal with EMC, namely, Part 15 (for radio-frequency systems), Part 18 (for industrial, scientific, and medical equipment), and Part 68 (for equipment connected to the telephone network). The standard regulations divide devices or equipment into two categories: Class A and Class B. Class A includes systems used in the commercial, industry, and business sectors, whereas Class B includes domestic systems. The regulation limits for Class B (approximately 10 dB) are stricter than those for Class A. All systems with digital circuits and a clock frequency above 10 kHz fall within the FCC regulations. The conducted interference limits are listed in the range of 450 kHz to 30 Hz, and the present limit controls the interference current in power leads. The leading organization for EMC standardization in the United States is the ANSI, to which various other institutions also contribute, such as the IEEE EMC Society [34, 35].

1.5.3 European Standards

The European Standard Committee (ESC) monitors the regulation and implantation of suitable standards using CENELEC. These standards, including basic standards (test methods) and product standards (specific types of equipment), classify systems or equipment into broad classes, namely, class 1 (residential and light industrial) and class 2 (heavy industry). The mandate of 3 May 1989, related to EMC prerequisites, was amended for a transitional period and came into effect on 1 January 1996. All the member nations have to sanction the legislation to implement these orders. The standard orders are widely inclusive, accounting for the emission and susceptibility of various hardware or systems and imposing duties on the manufacturers, irrespective of the existence of suitable guidelines. A trade agreement was signed in 1997 between the FCC and CENELEC, through which any EMC test conducted in either the United States or the EU is acknowledged by both parties. Thus, trade barriers were demolished, and both European and US manufacturing companies and testing laboratories can export and import equipment to each other [34].

1.5.4 Korean Standards

Korean EMC and safety standards are implanted and maintained by the Radio Research Agency (RRA) and the Korean Agency for Technology and Standards (KATS). The standards are classified into two categories: EMC (Radio Wave Law) and safety (Electric Appliances Safety Control Act). The first EMC policy was converted into the Radio Wave Act in 1989, and the electromagnetic susceptibility (immunity) criteria were enforced in 2000. The Korean EMC standards (KS) are identical to the IEC standards. For example, the KN 61000-6 family of standards is identical to the IEC 61000 standards. The KN 14 standard, which deals with household and electrical systems, is analogous to the CISPR 14-1 standard. Moreover, all products that meet Korean EMC and electrical safety requirements are engraved with a KC mark before being introduced to the Korean market. In July 2011, the EU and Korea established a system that facilitates the certification processes for electrical and electronic systems, thus increasing market accessibility.

1.5.5 Military or Defense Standards

The most important group of EMC standards is the military standards. In modern warfare, electric and electronic communications are used to set up integrated control commands among all the forces (land, air, and sea). Hostile warfare requires compact and confidential systems. Moreover, the high use of electromagnetic energy for jamming has generated critical EMC systems and EMI complications. Any electrical system designed and developed for defense purposes must fulfill the MIL-STD-461 standard, which gives a limit range for the susceptibility of equipment to conduct and radiate EMI. The MIL-STD-462 companion standard provides testing procedures. Moreover, the MIL-STD-461 standards have been acknowledged and implemented outside the United States by various defense establishments and a few nonmilitary organizations. Military equipment should be able to withstand radiated and conducted RF without malfunctioning. The military standards are stricter than the civilian standards (FCC, ESC, and CISPR22) as they deal with both susceptibility and emission and cover a frequency range of 30–40 GHz. Strict military standards are needed for radiated emission because of the small size of the working space, where electronic systems are kept in close proximity in fighter jets, tanks, naval ships, etc. In contrast, these systems can be more widely distributed in industrial installations [34, 35].

1.6 Materials for EMI Shielding

The rise of electronic and electrical devices started after the development of the electromagnetic theory in the nineteenth century. The understanding of the electromagnetic theory has led to the use of EMWs for wireless communication, information sharing and broadcasting, foreign object detection by security systems, and medical applications and imaging. In general, every device currently working on a power source receives or generates undesirable EMWs. Devices operating in close proximity can interfere with each other, resulting in malfunctioning or failure and can also affect human health. Therefore, in this advanced technology era, as we cannot reduce the use of electronic equipment, huge efforts are being made to develop efficient materials to mitigate or absorb the energy of undesirable EMWs.

As mentioned previously, reflection is the primary mechanism of EMI shielding, as a major portion of the incident EMWs is reflected after striking the surface of a shielding material. In this regard, highly conductive metals (e.g. Ag, Cu, and Al) in the form of foils or shrouds have been commonly used for decades as potential EMI shielding materials [2]. Owing to their high electrical conductivities of 10^5–10^6 S cm^{-1}, these metals have abundant free electrons that can interact with the incident EMWs and reflect them back into space. The excellent thermal conductivities of these metals (200–500 W m^{-1} K^{-1}) also expand their applications. However, the shielding performance of highly conductive metals is outweighed by various drawbacks such as high density, high cost, poor corrosion resistance, and difficulties in processing at smaller thicknesses. These factors limit the applications of metals in the aircraft and aerospace industry, where lightweight materials are a priority. Moreover, the reflection mechanism generates secondary pollution when the reflected EMWs interact with surrounding circuits. Therefore, in advanced portable and smart devices, efficient absorbing materials are being extensively explored.

Although electrical conductivity is a critical parameter for determining the performance of an EMI shielding material, it is not the only factor. Ferromagnetic materials (paramagnetic materials) show strong absorption behavior owing to spontaneous magnetization below the Curie temperature [36]. Under an applied magnetic field, the spin moments in the domains (a microscopically large homogeneous region) are aligned parallel to the magnetic field, resulting in the storage of the energy associated with electromagnetic radiation. Thus, the magnetic permeability of a material is an important criterion for defining the ability of the material to absorb the energy of EMWs. As a result, ferrites have become of significant academic and industrial interest to overcome the disadvantages of highly conductive metals.

Conductive polymer nanocomposites with metal nanoparticles and ferrite inclusions have excellent capabilities for EMI shielding. In particular, cost-effective and easily processable composites with multiphase heterogeneous structures hosting carbon nanotubes (CNTs) or carbon black (CB) have received considerable attention.

Currently, two-dimensional (2D) nanomaterials are at the forefront of ongoing research owing to their unique chemical, mechanical, electrical, and optoelectronic properties [37–41]. Since the discovery of graphene in 2004, research on 2D materials has proceeded at a far higher rate than ever before [42]. Nevertheless, this field is still emerging, with new materials being discovered every year and many more anticipated in the future. The range of 2D materials includes graphene [5, 43–45], black phosphorous (BP), [46] hexagonal boron nitride (h-BN) [47], transition metal dichalcogenides (TMDCs; e.g. MoS_2, WS_2, TaS_2, $MoSe_2$, and WSe_2), [48–50] and the very new yet gigantic family of transition metal carbides/nitrides/carbonitrides (MXenes; e.g. $Ti_3C_2T_x$, Ti_3CNT_x, and Ti_2CT_x) [51–54]. The development of novel 2D materials beyond graphene has revealed a wide range of electrical conductivities (0.004–15 000 S cm^{-1}, Table 1.1), which imparts extraordinary potential for diverse applications in almost all technological areas. Owing to their excellent electrical conductivity, processability, corrosion resistance, and low density, 2D materials are believed to be an alternative to highly conductive metals for EMI shielding. Monolayer graphene shows outstanding EMI shielding potential because of its very high electrical conductivity (5.25×10^4 S cm^{-1}) in chemical vapor deposition

Table 1.1 Fundamental properties of conventional shielding materials and advanced 2D nanomaterials.

Material		Properties							
		Conductivity ($S\,cm^{-1}$)	Permeability (μ′/μ″)	Carrier density (cm^{-3})	Carrier mobility ($cm^2\,V^{-1}\,s^{-1}$)	Density ($g\,cm^{-3}$)	Thermal conductivity ($W\,m^{-1}\,K^{-1}$)	Electronic bandgap (eV)	References
Metals	Silver	6.305×10^5	—	5.86×10^{22}	9490	10.53	417–427	N/A	[55, 56]
	Copper	5.977×10^5	—	8.47×10^{22}	5770	8.9	386–400	N/A	[55, 56]
	Aluminum	3.538×10^5	—	18.1×10^{22}	2600	2.7	234	N/A	[55, 56]
Magnetic materials	Fe_2O_3	3.12×10^{-7}	1.2/0.8(4 GHz, 70 wt%/wax)	1.65×10^{19}	$\sim 10^{-2}$	5.25	—	2.0–2.4	[57–64]
	Fe_3O_4	$\sim 10^2$–10^3	1.4/0.9 (4 GHz, 70 wt%/wax)	4.04×10^{22}	—	5.17	2.7 (cross) 2.6 (in-plane)	2.3	[57, 58, 60, 63–70]
	Sendust	1.397	4/1.5 (1 GHz, 40 vol%/acryl)	—	—	2.4–3.5	1.83 (50 vol%/PP)	—	[71–73]
	Permalloy	0.8	9/8 (1 GHz, 70 vol%/PPS)	$7.9 \times 10^{11}\ cm^{-2}$	0.5×10^6	8.7	19	—	[74–76]
	MnZn ferrite	0.008 (71 vol%/PANI)	3/4 (1 GHz, 71 vol%/PANI)	—	—	4.8	4	2.19	[76–78]
	NiZn ferrite	1.35×10^{-1} (54 wt%/PANI)	1–2/7–8 (1 GHz)	—	—	5.2	7	1.91	[76, 79–82]
2D materials	Graphene CVD graphene	5.25×10^4	—	2.8×10^{13}	4.4×10^4	—	2500 ± 1000	0.01	[83–89]
	Graphene oxide	(Insulating)	—	—	0.25	2.2	776	1.7	[90–93]
	Reduced graphene oxide	7–205	—	1.3×10^{11}	16–262	2.1	1390	2.2–0.5	[94–101]

	S-doped graphene	21–311	—	2.3×10^{18}	60–270	2.25	N/A	0.1–0.2	[99, 102–104]
	N-doped graphene	12–316	—	2.5×10^{15} (N-doped) 6×10^{14} (B-doped)	350–550 (N-doped) 450–650 (B-doped)	~2	4–300 (N-doped) 190 (B-doped)	0.2 eV (N-doped) 0.6 eV (N,B-codoping)	[105–113]
MXenes	$Ti_3C_2T_x$	5000–15 000	—	$(2.6–3.2) \times 10^{16}$ cm^{-2}	(0.6–1.25)	2.39	2.84	0.5–2	[114]
	Ti_3CNT_x	1125–2712	—	—	—	—	—	—	[4, 115]
	Ti_2CT_x	1600–2000	—	1×10^{22}	33.6×10^3	~2	11.91	0.88–1.15	[116–119]
	V_2CT_x	998–1560	—	—	—	—	—	—	[115]
	Nb_2CT_x	5	—	—	$\sim 1 \times 10^6$	—	15	—	[115, 120, 121]
	Mo_2CT_x	0.017–4.3	—	—	—	—	48.4	—	[122]
	Sc_2CF_2	—	—	—	$(1.07–5.03) \times 10^3$	—	178–472	1.03	[119, 123]
	$Sc_2C(OH)_2$	—	—	—	$(2.06–2.19) \times 10^3$	—	107–173	0.45	[119, 123]
TMDCs	MoS_2	1000	—	2.6×10^{12} cm^{-2}	50–217	5.06	34.5–131	1.3 (indirect)	[124–131]
	WS_2	6.7	—	1.0×10^{17} cm^{-2} (thin film) $3.0 \times 10^{17} \sim 1.6 \times 10^{18}$ cm^{-3} (nanotube)	0.2	7.5	32 (monolayer) 53 (bilayer)	1.35 (bulk) 2.05 (monolayer)	[131–137]
	TaS_2	680	—	4.5×10^{19} cm^{-3}	20	6.86	11.55–13.36	0.3	[138–141]
Others	CuS	870	—	2.09×10^{21} cm^{-3}	1–6	4.76	1.8	2.0	[142–145]
	h-BN	(Insulating)	—	—	2300	2.28	280	4.9–6.4	[146, 147]
	BP	0.004	—	2.6×10^{14} cm^{-2}	1000	2.69	110 (AC) 35 (ZZ)	0.3 (bulk) 2.0 (monolayer)	[148–156]

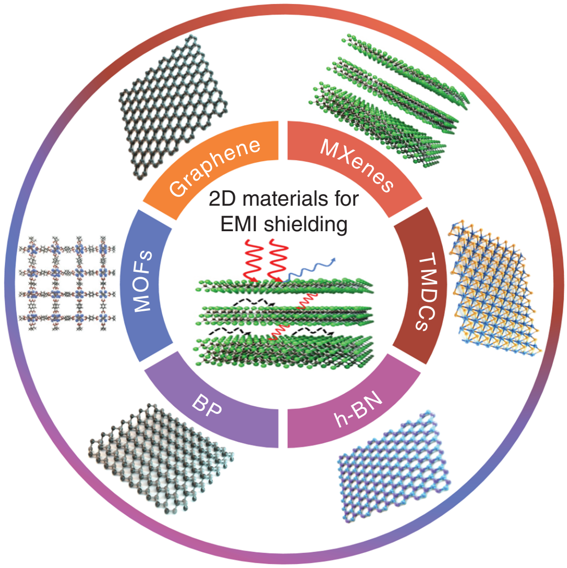

Figure 1.5 Atomic structures of 2D materials used for EMI shielding. The development of these novel 2D materials has provided a breakthrough in replacing conventional conductive metals, which suffer from high density and corrosion susceptibility. Source: Chong Min Koo.

(CVD)-grown nanometer thin films. At higher thicknesses, the electrical conductivity decreases because the defect concentration increases. Metallic conductivities of more than 15 000 S cm^{-1} have been achieved for MXenes at thicknesses of nanometers to tens of micrometers, and their polymeric composites show an ultralow percolation threshold with superior electrical conductivity. Owing to their unique advantages for fabricating highly processable liquid dispersions, inks, low-percolation polymer composites, and flexible and lightweight composites, 2D materials can satisfy the requirements for on-ground and space applications. TMDCs with 2D morphologies, including WS_2, TaS_2, and MoS_2, show high electrical conductivities of 6.7, 680, and 1000 S cm^{-1}, respectively. CuS, another 2D material, also exhibits a high electrical conductivity of 870 S cm^{-1}. The synergistic effect of efficient electrical conductivity and a multilayered morphology makes these 2D materials effective for practical EMI shielding applications. The fundamental properties of conventional and novel EMI shielding materials are summarized in Table 1.1, and these materials, especially 2D graphene, MXenes, TMDCs, BP, h-BN, and MOF (Figure 1.5), are discussed in detail in Chapters 4–6.

The current rise in 5G technology demands more efficient EMI shielding materials with ultralow densities and thicknesses. The area of EMI shielding materials is emerging parallel to technological advancements, and scientists are using a structural control approach to further enhance and tailor the properties of 2D materials according to the desired area of application. In this way, compact solid films and composites, porous foams and aerogels, and segregated structures have been developed for use as thin, strong, lightweight, and cost-effective shielding materials [11].

1.7 Summary

The rapid advancement of highly integrated electronic, telecom, defense, and medical devices has resulted in serious EMI, which can detrimentally impact the performance and lifetime of these devices as well as human health. Although metals and magnetic materials have long been used for EMI shielding, they are not a good choice for lightweight and portable technologies. Novel 2D materials, which possess high electrical conductivity, low density, high mechanical strength, and excellent EMI SE at a minimal thickness, can provide the same EMI shielding performance as metals while minimizing the drawbacks. The shielding and absorption of EMWs is pivotal in a wide variety of industries, including satellites, aerospace, and defense, which provide a huge global market for EMI shielding and absorbing materials. Therefore, efficient materials with the required set of fundamental properties are highly needed, and thus continue to be explored. This book provides insights into the potential of 2D materials for lightweight EMI shielding.

References

1 Simon, R.M. (1981). EMI shielding through conductive plastics. *Polymer-Plastics Technology and Engineering* 17 (1): 1–10.

2 Shahzad, F., Alhabeb, M., Hatter, C.B. et al. (2016). Electromagnetic interference shielding with 2D transition metal carbides (MXenes). *Science* 353 (6304): 1137–1140.

3 Chen, Z., Xu, C., Ma, C. et al. (2013). Lightweight and flexible graphene foam composites for high-performance electromagnetic interference shielding. *Advanced Materials* 25 (9): 1296–1300.

4 Iqbal, A., Shahzad, F., Hantanasirisakul, K. et al. (2020). Anomalous absorption of electromagnetic waves by 2D transition metal carbonitride Ti_3CNT_x (MXene). *Science* 369 (6502): 446–450.

5 Hong, S.K., Kim, K.Y., Kim, T.Y. et al. (2012). Electromagnetic interference shielding effectiveness of monolayer graphene. *Nanotechnology* 23 (45): 455704.

6 Lee, C., Lee, D., Jeong, C. et al. (2002). Electromagnetic interference shielding by using conductive polypyrrole and metal compound coated on fabrics. *Polymers for Advanced Technologies* 13 (8): 577–583.

7 Geetha, S., Satheesh Kumar, K., Rao, C.R. et al. (2009). EMI shielding: methods and materials—a review. *Journal of Applied Polymer Science* 112 (4): 2073–2086.

8 Nazir, A., Yu, H., Wang, L. et al. (2018). Recent progress in the modification of carbon materials and their application in composites for electromagnetic interference shielding. *Journal of Materials Science* 53 (12): 8699–8719.

9 Stam, R. and Yamaguchi-Sekino, S. (2018). Occupational exposure to electromagnetic fields from medical sources. *Industrial Health* 56 (2): 96–105.

10 Gurevich, V. (2005). The hazards of electromagnetic terrorism. *Public Utilities Fortnightly* 143: 84–86.

11 Iqbal, A., Sambyal, P., and Koo, C.M. (2020). 2D MXenes for electromagnetic shielding: a review. *Advanced Functional Materials* 30: 2000883.

12 Yun, T., Kim, H., Iqbal, A. et al. (2020). Electromagnetic shielding of monolayer MXene assemblies. *Advanced Materials* 32 (9): 1906769.

13 Lee, S.H., Yu, S., Shahzad, F. et al. (2017). Density-tunable lightweight polymer composites with dual-functional ability of efficient EMI shielding and heat dissipation. *Nanoscale* 9 (36): 13432–13440.

14 Choi, Y.-S., Yoo, Y.-H., Kim, J.-G. et al. (2006). A comparison of the corrosion resistance of Cu–Ni–stainless steel multilayers used for EMI shielding. *Surface and Coatings Technology* 201 (6): 3775–3782.

15 De Temmerman, L. (1992). New metallized materials for EMI/RFI shielding. *Journal of Coated Fabrics* 21 (3): 191–198.

16 Luo, X. and Chung, D. (1999). Electromagnetic interference shielding using continuous carbon-fiber carbon-matrix and polymer-matrix composites. *Composites Part B Engineering* 30 (3): 227–231.

17 Kim, S.-S., Kim, S.-T., Yoon, Y.-C. et al. (2005). Magnetic, dielectric, and microwave absorbing properties of iron particles dispersed in rubber matrix in gigahertz frequencies. *Journal of Applied Physics* 97 (10): 10F905.

18 Bhadra, S., Singha, N.K., and Khastgir, D. (2009). Dielectric properties and EMI shielding efficiency of polyaniline and ethylene 1-octene based semi-conducting composites. *Current Applied Physics* 9 (2): 396–403.

19 Yin, X., Xue, Y., Zhang, L. et al. (2012). Dielectric, electromagnetic absorption and interference shielding properties of porous yttria-stabilized zirconia/silicon carbide composites. *Ceramics International* 38 (3): 2421–2427.

20 Chen, Y., Zhang, H.-B., Huang, Y. et al. (2015). Magnetic and electrically conductive epoxy/graphene/carbonyl iron nanocomposites for efficient electromagnetic interference shielding. *Composites Science and Technology* 118: 178–185.

21 Bosman, H., Lau, Y.Y., and Gilgenbach, R.M. (2003). Microwave absorption on a thin film. *Applied Physics Letters* 82 (9): 1353–1355.

22 Bren, S.A. (1996). Historical introduction to EMF health effects. *IEEE Engineering in Medicine and Biology Magazine* 15 (4): 24–30.

23 Jaroszewski, M., Thomas, S., and Rane, A.V. (2018). *Advanced Materials for Electromagnetic Shielding: Fundamentals, Properties, and Applications*. Wiley.

24 Singh, M. (2014). *Introduction to Biomedical Instrumentation*. PHI Learning Pvt. Ltd.

25 Hansson Mild, K.; Repacholi, M.; Van Deventer, E.; Ravazzani, P. et al. (2004). Electromagnetic hypersensitivity: proceedings. *International Workshop on EMF Hypersensitivity*, Prague, Czech Republic.

26 Singh, S. and Kapoor, N. (2014). Health implications of electromagnetic fields, mechanisms of action, and research needs. *Advances in Biology* 2014: 198609.

27 Van Wijngaarden, E., Savitz, D.A., Kleckner, R.C. et al. (2000). Exposure to electromagnetic fields and suicide among electric utility workers: a nested case-control study. *Occupational and Environmental Medicine* 57 (4): 258–263.

28 Budak, B., Budak, G.G., Öztürk, G.G. et al. (2009). Effects of extremely low frequency electromagnetic fields on distortion product otoacoustic emissions in rabbits. *Auris Nasus Larynx* 36 (3): 255–262.

29 Wessapan, T. and Rattanadecho, P. (2013). Specific absorption rate and temperature increase in the human eye due to electromagnetic fields exposure at different frequencies. *International Journal of Heat and Mass Transfer* 64: 426–435.

30 Ghione, S., Del Seppia, C., Mezzasalma, L. et al. (2004). Human head exposure to a 37 Hz electromagnetic field: effects on blood pressure, somatosensory perception, and related parameters. *Bioelectromagnetics* 25 (3): 167–175.

31 Erpek, S., Bilgin, M.D., Dikicioglu, E. et al. (2007). The effects of low frequency electric field in rat testis. *Revue de Médecine Vétérinaire* 158 (4): 206–212.

32 EMI shielding market by material (EMI shielding tapes & laminates, conductive coatings & paints, metal shielding, conductive polymers, EMI filters), method (radiation, conduction), industry, and region – global forecast to 2025. https://www.marketsandmarkets.com/Market-Reports/emi-shielding-market-105681800.html#:~:text=%5B143%20Pages%20Report%5D%20The%20globalwww.marketsandmarkets.com (accessed 7 January 2021).

33 Celozzi, S., Araneo, R., and Lovat, G. (2008). *Electromagnetic Shielding*. Wiley.

34 Tong, X.C. (2016). *Advanced Materials and Design for Electromagnetic Interference Shielding*. CRC Press.

35 Ott, H.W. (1976). *Noise Reduction Techniques in Electronic Systems*. Wiley.

36 Sasaki, T., Sonoda, S., Yamamoto, Y. et al. (2002). Magnetic and transport characteristics on high curie temperature ferromagnet of Mn-doped GaN. *Journal of Applied Physics* 91 (10): 7911–7913.

37 Zhang, H. (2015). Ultrathin two-dimensional nanomaterials. *ACS Nano* 9 (10): 9451–9469.

38 Khan, K., Tareen, A.K., Aslam, M. et al. (2020). Recent developments in emerging two-dimensional materials and their applications. *Journal of Materials Chemistry C* 8 (2): 387–440.

39 Stanford, M.G., Rack, P.D., and Jariwala, D. (2018). Emerging nanofabrication and quantum confinement techniques for 2D materials beyond graphene. *NPJ 2D Materials and Applications* 2 (1): 20.

40 Zavabeti, A., Jannat, A., Zhong, L. et al. (2020). Two-dimensional materials in large-areas: synthesis, properties and applications. *Nano-Micro Letters* 12 (1): 66.

41 Hantanasirisakul, K. and Gogotsi, Y. (2018). Electronic and optical properties of 2D transition metal carbides and nitrides (MXenes). *Advanced Materials* 30 (52): 1804779.

42 Novoselov, K.S., Geim, A.K., Morozov, S.V. et al. (2004). Electric field effect in atomically thin carbon films. *Science* 306 (5696): 666–669.

43 Jia, L.-C., Yan, D.-X., Liu, X. et al. (2018). Highly efficient and reliable transparent electromagnetic interference shielding film. *ACS Applied Materials & Interfaces* 10 (14): 11941–11949.

44 Erdogan, N., Erden, F., Astarlioglu, A.T. et al. (2020). ITO/Au/ITO multilayer thin films on transparent polycarbonate with enhanced EMI shielding properties. *Current Applied Physics* 20 (4): 489–497.

45 Wang, H., Lu, Z., Liu, Y. et al. (2017). Double-layer interlaced nested multi-ring array metallic mesh for high-performance transparent electromagnetic interference shielding. *Optics Letters* 42 (8): 1620–1623.

46 Hanlon, D., Backes, C., Doherty, E. et al. (2015). Liquid exfoliation of solvent-stabilized few-layer black phosphorus for applications beyond electronics. *Nature Communications* 6 (1): 1–11.

47 Lin, Y., Williams, T.V., and Connell, J.W. (2010). Soluble, exfoliated hexagonal boron nitride nanosheets. *The Journal of Physical Chemistry Letters* 1 (1): 277–283.

48 Chhowalla, M., Shin, H.S., Eda, G. et al. (2013). The chemistry of two-dimensional layered transition metal dichalcogenide nanosheets. *Nature Chemistry* 5 (4): 263–275.

49 Huang, X., Zeng, Z., and Zhang, H. (2013). Metal dichalcogenide nanosheets: preparation, properties and applications. *Chemical Society Reviews* 42 (5): 1934–1946.

50 Chhowalla, M., Liu, Z., and Zhang, H. (2015). Two-dimensional transition metal dichalcogenide (TMD) nanosheets. *Chemical Society Reviews* 44 (9): 2584–2586.

51 Naguib, M., Kurtoglu, M., Presser, V. et al. (2011). Two-dimensional nanocrystals produced by exfoliation of Ti_3AlC_2. *Advanced Materials* 23 (37): 4248–4253.

52 Naguib, M., Mashtalir, O., Carle, J. et al. (2012). Two-dimensional transition metal carbides. *ACS Nano* 6 (2): 1322–1331.

53 Anasori, B., Xie, Y., Beidaghi, M. et al. (2015). Two-dimensional, ordered, double transition metals carbides (MXenes). *ACS Nano* 9 (10): 9507–9516.

54 Anasori, B. and Gogotsi, Û.G. (2019). *2D Metal Carbides and Nitrides (MXenes)*. Springer.

55 Huang, Y., Kormakov, S., He, X. et al. (2019). Conductive polymer composites from renewable resources: an overview of preparation, properties, and applications. *Polymers* 11 (2): 187.

56 Palenskis, V. (2013). Drift mobility, diffusion coefficient of randomly moving charge carriers in metals and other materials with degenerated electron gas. *World Journal of Condensed Matter Physics* 3: 73–81.

57 Meng, Y., Liu, X.-W., Huo, C.-F. et al. (2016). When density functional approximations meet iron oxides. *Journal of Chemical Theory and Computation* 12 (10): 5132–5144.

58 Sivakumar, G. (2017). Synthesis of γ-Fe_2O_3, Fe_3O_4 and copper doped Fe_3O_4 nanoparticles by sonochemical method. *Sains Malaysiana* 46 (10): 1935–1942.

59 Gao, Y., Wu, D., Wang, T. et al. (2016). One-step solvothermal synthesis of quasi-hexagonal Fe_2O_3 nanoplates/graphene composite as high performance electrode material for supercapacitor. *Electrochimica Acta* 191: 275–283.

60 Wu, H., Wu, G., and Wang, L. (2015). Peculiar porous α-Fe_2O_3, γ-Fe_2O_3 and Fe_3O_4 nanospheres: facile synthesis and electromagnetic properties. *Powder Technology* 269: 443–451.

61 Cheng, F. and Li, X. (2020). Effects of in situ Co or Ni doping on the photoelectrochemical performance of hematite nanorod arrays. *Applied Sciences* 10 (10): 3567.

62 Morin, F.J. (1954). Electrical properties of α-Fe_2O_3. *Physical Review* 93 (6): 1195.

63 Haynes, W. (2011). *CRC Handbook of Chemistry and Physics*, 92e. Boca Raton, FL: CRC Press/Taylor and Francis.

64 Sun, G., Dong, B., Cao, M. et al. (2011). Hierarchical dendrite-like magnetic materials of Fe_3O_4, γ-Fe_2O_3, and Fe with high performance of microwave absorption. *Chemistry of Materials* 23 (6): 1587–1593.

65 Lee, K.K., Deng, S., Fan, H.M. et al. (2012). α-Fe_2O_3 nanotubes-reduced graphene oxide composites as synergistic electrochemical capacitor materials. *Nanoscale* 4 (9): 2958–2961.

66 Hotta, M., Hayashi, M., and Nagata, K. (2011). High temperature measurement of complex permittivity and permeability of Fe_3O_4 powders in the frequency range of 0.2 to 13.5 GHz. *ISIJ International* 51 (3): 491–497.

67 Liu, X., Wing Or, S., Ming Leung, C. et al. (2013). Microwave complex permeability of Fe_3O_4 nanoflake composites with and without magnetic field-induced rotational orientation. *Journal of Applied Physics* 113 (17): 17B307.

68 Ramajo, L.A., Cristóbal, A.A., Botta, P.M. et al. (2009). Dielectric and magnetic response of Fe_3O_4/epoxy composites. *Composites Part A: Applied Science and Manufacturing* 40 (4): 388–393.

69 Radoń, A., Łukowiec, D., Kremzer, M. et al. (2018). Electrical conduction mechanism and dielectric properties of spherical shaped Fe_3O_4 nanoparticles synthesized by co-precipitation method. *Materials* 11 (5): 735.

70 Ramirez, S., Chan, K., Hernandez, R. et al. (2017). Thermal and magnetic properties of nanostructured densified ferrimagnetic composites with graphene – graphite fillers. *Materials and Design* 118: 75–80.

71 Oh, K.K., Lee, H., Lee, W.S. et al. (2009). Effect of viscosity on the magnetic permeability of Sendust-filled polymer composites. *Journal of Magnetism and Magnetic Materials* 321 (9): 1295–1299.

72 Tsutaoka, T., Ono, T., Tsurunaga, A. et al. (2011). High frequency permeability of Fe-Al-Si granular composite materials. In: *2011 IEEE International Symposium on Electromagnetic Compatibility*, 78–83. IEEE.

73 Lee, J., Nam, B., Ko, F.K. et al. (2015). Thermal conductivity prediction of magnetic composite sheet for near-field electromagnetic absorption. *AIP Journal of Applied Physics* 117 (17): 17C122.

74 Kasagi, T., Tsutaoka, T., and Hatakeyama, K. (2006). Negative permeability spectra in permalloy granular composite materials. *Applied Physics Letters* 88 (17): 172502.

75 Hengstmann, T., Grundler, D., Heyn, C. et al. (2001). Stray-field investigation on permalloy nanodisks. *AIP Journal of Applied Physics* 90 (12): 6542–6544.

76 Talaat, A., Greve, D.W., Suraj, M. et al. (2020). Electromagnetic assisted thermal processing of amorphous and nanocrystalline soft magnetic alloys: fundamentals and advances. *Journal of Alloys and Compounds* 854: 156480.

77 Babayan, V., Kazantseva, N.E., Sapurina, I. et al. (2013). Increasing the high-frequency magnetic permeability of MnZn ferrite in polyaniline composites by incorporating silver. *Journal of Magnetism and Magnetic Materials* 333: 30–38.

78 Farheen, A. and Singh, R. (2019). FMR and magnetic studies of RF-sputtered Mn-Zn ferrite thin films. *Journal of Superconductivity and Novel Magnetism* 32 (8): 2679–2686.

79 Brühl, M., Zhang, D., Talaka, T. et al. (2010). Microstructure and complex magnetic permeability of thermally sprayed NiZn ferrite coatings for electromagnetic wave absorbers. *Surface Engineering* 26 (6): 484–490.

80 Tsutaoka, T., Ueshima, M., Tokunaga, T. et al. (1995). Frequency dispersion and temperature variation of complex permeability of Ni-Zn ferrite composite materials. *AIP Journal of Applied Physics* 78 (6): 3983–3991.

81 Ali, N.N., Atassi, Y., Salloum, A. et al. (2018). Comparative study of microwave absorption characteristics of (polyaniline/NiZn ferrite) nanocomposites with different ferrite percentages. *Materials Chemistry and Physics* 211: 79–87.

82 Javed, H., Rehman, A., Mussadiq, S. et al. (2019). Reduced graphene oxide-spinel ferrite nano-hybrids as magnetically separable and recyclable visible light driven photocatalyst. *Synthetic Metals* 254: 1–9.

83 Deokar, G., Avila, J., Razado-Colambo, I. et al. (2015). Towards high quality CVD graphene growth and transfer. *Carbon* 89: 82–92.

84 Vlassiouk, I., Smirnov, S., Ivanov, I. et al. (2011). Electrical and thermal conductivity of low temperature CVD graphene: the effect of disorder. *Nanotechnology* 22 (27): 275716.

85 Sun, H., Ge, G., Zhu, J. et al. (2015). High electrical conductivity of graphene-based transparent conductive films with silver nanocomposites. *RSC Advances* 5 (130): 108044–108049.

86 Cai, W., Moore, A.L., Zhu, Y. et al. (2010). Thermal transport in suspended and supported monolayer graphene grown by chemical vapor deposition. *Nano Letters* 10 (5): 1645–1651.

87 Wang, L., Yin, M., Zhong, B. et al. (2019). Quantum transport properties of monolayer graphene with antidot lattice. *Journal of Applied Physics* 126 (8): 084305.

88 Petrone, N., Dean, C.R., Meric, I. et al. (2012). Chemical vapor deposition-derived graphene with electrical performance of exfoliated graphene. *Nano Letters* 12 (6): 2751–2756.

89 Kang, M.H., Qiu, G., Chen, B. et al. (2017). Transport in polymer-supported chemically-doped CVD graphene. *Journal of Materials Chemistry C* 5 (38): 9886–9897.

90 Venugopal, G., Krishnamoorthy, K., Mohan, R. et al. (2012). An investigation of the electrical transport properties of graphene-oxide thin films. *Materials Chemistry and Physics* 132 (1): 29–33.

91 Eda, G. and Chhowalla, M. (2010). Chemically derived graphene oxide: towards large-area thin-film electronics and optoelectronics. *Advanced Materials* 22 (22): 2392–2415.

92 Mahanta, N.K. and Abramson, A.R. (2012). Thermal conductivity of graphene and graphene oxide nanoplatelets. *13th InterSociety Conference on Thermal and Thermomechanical Phenomena in Electronic Systems.*

93 Jin, M., Jeong, H.-K., Yu, W.J. et al. (2009). Graphene oxide thin film field effect transistors without reduction. *Journal of Physics D: Applied Physics* 42 (13): 135109.

94 Chen, H., Müller, M.B., Gilmore, K.J. et al. (2008). Mechanically strong, electrically conductive, and biocompatible graphene paper. *Advanced Materials* 20 (18): 3557–3561.

95 Yang, H., Cao, Y., He, J. et al. (2017). Highly conductive free-standing reduced graphene oxide thin films for fast photoelectric devices. *Carbon* 115: 561–570.

96 Chang, H., Sun, Z., Yuan, Q. et al. (2010). Thin film field-effect phototransistors from bandgap-tunable, solution-processed, few-layer reduced graphene oxide films. *Advanced Materials* 22 (43): 4872–4876.

97 Kumar, P., Shahzad, F., Yu, S. et al. (2015). Large-area reduced graphene oxide thin film with excellent thermal conductivity and electromagnetic interference shielding effectiveness. *Carbon* 94: 494–500.

98 Gupta, S., Joshi, P., and Narayan, J. (2020). Electron mobility modulation in graphene oxide by controlling carbon melt lifetime. *Carbon* 170: 327–337.

99 Shahzad, F., Kumar, P., Kim, Y.-H. et al. (2016). Biomass-derived thermally annealed interconnected sulfur-doped graphene as a shield against electromagnetic interference. *ACS Applied Materials & Interfaces* 8 (14): 9361–9369.

100 Kajen, R., Chandrasekhar, N., Pey, K.L. et al. (2013). Charge transport in lightly reduced graphene oxide: a transport energy perspective. *Journal of Applied Physics* 113 (6): 063710.

101 Liang, C., Wang, Y., and Li, T. (2015). Synthesis of sulfur-doped p-type graphene by annealing with hydrogen sulfide. *Carbon* 82: 506–512.

102 Zhou, J., Wang, Z., Chen, Y. et al. (2017). Growth and properties of large-area sulfur-doped graphene films. *Journal of Materials Chemistry C* 5 (31): 7944–7949.

103 Denis, P.A. (2013). Concentration dependence of the band gaps of phosphorus and sulfur doped graphene. *Computational Materials Science* 67: 203–206.

104 Wang, Z., Li, P., Chen, Y. et al. (2014). Pure thiophene–sulfur doped reduced graphene oxide: synthesis, structure, and electrical properties. *Nanoscale* 6 (13): 7281–7287.

105 Usachov, D., Vilkov, O., Gruneis, A. et al. (2011). Nitrogen-doped graphene: efficient growth, structure, and electronic properties. *Nano Letters* 11 (12): 5401–5407.

106 Chang, C.-K., Kataria, S., Kuo, C.-C. et al. (2013). Band gap engineering of chemical vapor deposited graphene by in situ BN doping. *ACS Nano* 7 (2): 1333–1341.

107 Wu, T., Shen, H., Sun, L. et al. (2012). Nitrogen and boron doped monolayer graphene by chemical vapor deposition using polystyrene, urea and boric acid. *New Journal of Chemistry* 36 (6): 1385–1391.

108 Mann, S., Mudahar, I., Sharma, H. et al. (2020). Lattice thermal conductivity of pure and doped (B, N) graphene. *Materials Research Express* 7 (9): 095003.

109 Wang, H., Zhou, Y., Wu, D. et al. (2013). Synthesis of boron-doped graphene monolayers using the sole solid feedstock by chemical vapor deposition. *Small* 9 (8): 1316–1320.

110 Wang, Z., Li, P., Chen, Y. et al. (2014). Synthesis of nitrogen-doped graphene by chemical vapour deposition using melamine as the sole solid source of carbon and nitrogen. *Journal of Materials Chemistry C* 2 (35): 7396–7401.

111 Li, C., Hu, Y., Yu, M. et al. (2014). Nitrogen doped graphene paper as a highly conductive, and light-weight substrate for flexible supercapacitors. *RSC Advances* 4 (94): 51878–51883.

112 Arellano, L.M., Yue, S., Atienzar, P. et al. (2019). Modulating charge carrier density and mobility in doped graphene by covalent functionalization. *Chemical Communications* 55 (67): 9999–10002.

113 Kim, T.Y., Park, C.-H., and Marzari, N. (2016). The electronic thermal conductivity of graphene. *Nano Letters* 16 (4): 2439–2443.

114 Rajan, A.C., Mishra, A., Satsangi, S. et al. (2018). Machine-learning-assisted accurate band gap predictions of functionalized MXene. *Chemistry of Materials* 30 (12): 4031–4038.

115 Han, M., Shuck, C.E., Rakhmanov, R. et al. (2020). Beyond Ti_3C_2Tx: MXenes for electromagnetic interference shielding. *ACS Nano* 14 (4): 5008–5016.

116 Zhang, Y., Xia, W., Wu, Y. et al. (2019). Prediction of MXene based 2D tunable band gap semiconductors: GW quasiparticle calculations. *Nanoscale* 11 (9): 3993–4000.

117 Zha, X.-H., Huang, Q., He, J. et al. (2016). The thermal and electrical properties of the promising semiconductor MXene Hf_2CO_2. *Scientific Reports* 6 (1): 27971.

118 Jiang, X., Kuklin, A.V., Baev, A. et al. (2020). Two-dimensional MXenes: from morphological to optical, electric, and magnetic properties and applications. *Physics Reports* 848: 1–58.

119 Khazaei, M., Arai, M., Sasaki, T. et al. (2013). Novel electronic and magnetic properties of two-dimensional transition metal carbides and nitrides. *Advanced Functional Materials* 23 (17): 2185–2192.

120 Shao, Y., Zhang, F., Shi, X. et al. (2017). N-Functionalized MXenes: ultrahigh carrier mobility and multifunctional properties. *Physical Chemistry Chemical Physics* 19 (42): 28710–28717.

121 Huang, Y., Zhou, J., Wang, G. et al. (2019). Abnormally strong electron–phonon scattering induced unprecedented reduction in lattice thermal conductivity of two-dimensional Nb_2C. *Journal of the American Chemical Society* 141 (21): 8503–8508.

122 Zha, X.-H., Yin, J., Zhou, Y. et al. (2016). Intrinsic structural, electrical, thermal, and mechanical properties of the promising conductor Mo_2C MXene. *The Journal of Physical Chemistry C* 120 (28): 15082–15088.

123 Zha, X.-H., Zhou, J., Zhou, Y. et al. (2016). Promising electron mobility and high thermal conductivity in Sc_2CT_2 (T = F, OH) MXenes. *Nanoscale* 8 (11): 6110–6117.

124 Kobayashi, K. and Yamauchi, J. (1995). Electronic structure and scanning-tunneling-microscopy image of molybdenum dichalcogenide surfaces. *Physical Reviews B* 51 (23): 17085.

125 Yun, W.S., Han, S., Hong, S.C. et al. (2012). Thickness and strain effects on electronic structures of transition metal dichalcogenides: 2H-MX_2 semiconductors (M = Mo, W; X = S, Se, Te). *Physical Reviews B* 85 (3): 033305.
126 Worsley, M.A., Shin, S.J., Merrill, M.D. et al. (2015). Ultralow density, monolithic WS_2, MoS_2, and MoS_2/graphene aerogels. *ACS Nano* 9 (5): 4698–4705.
127 Pearce, C.I., Pattrick, R.A., and Vaughan, D.J.J.R.i.M. (2006). et al., Electrical and magnetic properties of sulfides. *Reviews in Mineralogy and Geochemistry* 61 (1): 127–180.
128 Fuhrer, M.S. and Hone, J. (2013). Measurement of mobility in dual-gated MoS_2 transistors. *Nature Nanotechnology* 8 (3): 146–147.
129 Kim, S., Hwang, W.-S., Lee, J.H. et al. (2012). High-mobility and low-power thin-film transistors based on multilayer MoS_2 crystals. *Nature Communications* 3 (1): 1–7.
130 Joo, M.-K., Moon, B.H., Ji, H. et al. (2016). Electron excess doping and effective Schottky barrier reduction on the MoS_2/h-BN heterostructure. *Nano Letters* 16 (10): 6383–6389.
131 Balach, J., Linnemann, J., Jaumann, T., and Giebeler, L.J.J.o.M.C.A. (2018). et al., Metal-based nanostructured materials for advanced lithium–sulfur batteries. *Journal of Materials Chemistry A* 6 (46): 23127–23168.
132 Velický, M. and Toth, P.S. (2017). From two-dimensional materials to their heterostructures: an electrochemist's perspective. *Applied Materials Today* 8: 68–103.
133 Eagleson, M. (1994). *Concise Encyclopedia Chemistry*. Walter de Gruyter.
134 Baglio, J.A., Calabrese, G.S., Kamieniecki, E. et al. (1982). Characterization of n-type semiconducting tungsten disulfide photoanodes in aqueous and non-aqueous electrolyte solutions: photo-oxidation of halides with high efficiency. *Journal of Electrochemical Society* 129 (7): 1461.
135 Gutiérrez, H.R., Perea-López, N., Elías, A.L. et al. (2013). Extraordinary room-temperature photoluminescence in triangular WS_2 monolayers. *Nano Letters* 13 (8): 3447–3454.
136 Zhang, C., Ning, Z., Liu, Y. et al. (2012). Electrical transport properties of individual WS_2 nanotubes and their dependence on water and oxygen absorption. *AIP Applied Physics Letters* 101 (11): 113112.
137 Peimyoo, N., Shang, J., Yang, W. et al. (2015). Thermal conductivity determination of suspended mono- and bilayer WS_2 by Raman spectroscopy. *Nano Research* 8 (4): 1210–1221.
138 Li, L., Deng, X., Wang, Z. et al. (2017). Superconducting order from disorder in 2H-$TaSe_{2-x}S_x$. *npj Quantum Materials* 2 (1): 1–7.
139 Sunilkumar, A., Manjunatha, S., Chethan, B. et al. (2019). Polypyrrole–tantalum disulfide composite: an efficient material for fabrication of room temperature operable humidity sensor. *Sensors and Actuators A: Physical* 298: 111593.
140 Hollander, M.J., Liu, Y., Lu, W.-J. et al. (2015). Electrically driven reversible insulator–metal phase transition in 1T-TaS_2. *Nano Letters* 15 (3): 1861–1866.
141 Çakıroğlu, O., Mehmood, N., Çiçek, M.M. et al. (2020). Thermal conductivity measurements in nanosheets via bolometric effect. *2D Materials* 7 (3): 035003.

142 Sun, K., Su, D., Zhang, Q. et al. (2015). Interaction of CuS and sulfur in Li-S battery system. *Journal of the Electrochemical Society* 162 (14): A2834.
143 Chloob, M.K. and Hussain, S.A. (2020). Study the structural and optical properties pure copper sulfide (CuS) films prepared by pulsed laser deposition (PLD). *Journal of Physics: Conference Series* 1591: 012014.
144 Kar, P., Farsinezhad, S., Zhang, X. et al. (2014). Anodic Cu_2S and CuS nanorod and nanowall arrays: preparation, properties and application in CO_2 photoreduction. *Nanoscale* 6 (23): 14305–14318.
145 Maneesha, P., Paulson, A., Muhammed Sabeer, N.A. et al. (2018). Thermo electric measurement of nanocrystalline cobalt doped copper sulfide for energy generation. *Materials Letters* 225: 57–61.
146 Sahoo, S.K. and Wei, K.H. (2019). A perspective on recent advances in 2D stanene nanosheets. *Advanced Materials Interfaces* 6 (18): 1900752.
147 Zhang, J., Tu, R., Goto, T.J.J.o.a. et al. (2010). Preparation of Ni-precipitated hBN powder by rotary chemical vapor deposition and its consolidation by spark plasma sintering. *Journal of Alloys and Compounds* 502 (2): 371–375.
148 Li, L., Yu, Y., Ye, G.J. et al. (2014). Black phosphorus field-effect transistors. *Nature Nanotechnology* 9 (5): 372.
149 Jain, A. and McGaughey, A.J.H. (2015). Strongly anisotropic in-plane thermal transport in single-layer black phosphorene. *Scientific Reports* 5: 8501.
150 Qiao, J., Kong, X., Hu, Z.-X. et al. (2014). et al., High-mobility transport anisotropy and linear dichroism in few-layer black phosphorus. *Nature Communications* 5 (1): 1–7.
151 Zhang, G., Huang, S., Chaves, A. et al. (2017). et al., Infrared fingerprints of few-layer black phosphorus. *Nature Communications* 8 (1): 1–9.
152 Tran, V., Soklaski, R., Liang, Y. et al. (2014). Layer-controlled band gap and anisotropic excitons in few-layer black phosphorus. *Physical Review B* 89 (23): 235319.
153 Saito, Y. and Iwasa, Y. (2015). Ambipolar insulator-to-metal transition in black phosphorus by ionic-liquid gating. *ACS Nano* 9 (3): 3192–3198.
154 Liu, C., Li, H., Xu, H. et al. (2019). Slow light effect based on tunable plasmon-induced transparency of monolayer black phosphorus. *Journal of Physics D: Applied Physics* 52 (40): 405203.
155 Low, T., Engel, M., Steiner, M. et al. (2014). Origin of photoresponse in black phosphorus phototransistors. *Physical Review B* 90 (8): 081408.
156 Liu, H., Du, Y., Deng, Y. et al. (2015). Semiconducting black phosphorus: synthesis, transport properties and electronic applications. *Chemical Society Reviews* 44 (9): 2732–2743.